Journal of Environmental Chemical Engineering 11 (2023) 109671

Contents lists available at ScienceDirect

Journal of Environmental Chemical Engineering

journal homepage: www.elsevier.com/locate/jece

Microplastics profile in sludge from a university wastewater treatment plant and the influence of chemical digestions on Nile red stained microplastics

Zhiqiang Gao [a], James V. Cizdziel [a,*], Laiguo Chen [b]

[a] Department of Chemistry and Biochemistry, University of Mississippi, University, MS 38677, USA
[b] Guangdong Provincial Key Laboratory of Water and Air Pollution Control, South China Institute of Environmental Sciences, MEE, Guangzhou 510655, China

ARTICLE INFO

Editor: Stefanos Giannakis

Keywords:
Microplastics
Digestion
Sewage sludge
University
Wastewater treatment plant

ABSTRACT

Many of the microplastics (MPs) entering wastewater treatment plants (WWTPs) become entrained in the waste sludge. Here, we assessed the effects of five common digestion methods on the degradation and fluorescence intensity of Nile-red stained MPs. Crumb rubber (CR), cellulose acetate (CA) and polyamide (PA) dissolved in an acid-based digestion; Polyethylene terephthalate (PET), polylactic acid (PLA) and CA degraded in alkali solutions; and CR was destroyed by 30 % H_2O_2. Fenton's reagent resulted in little to no damage to the polymers and removed > 95 % of the organic matter, making it the best choice for MP analyses. We then applied Fenton's reagent to extract MPs in the primary sludge and dewatered sludge from a modern WWTP at the University of Mississippi. There is limited research on MPs in university WWTPs, where the wastewater inflows and composition vary greatly depending on activities and populations on campus. Abundances of putative MPs ranged from 13.2 ± 3.8–380.0 ± 46.4 particles/g (dry weight), with higher levels in the primary sludge and dewatered sludge with students on campus. The majority of MPs were fibers < 500 μm. Over 20 polymers were identified by using μ-FTIR, with polyester (26.4 %), nylon (14.9 %), and polyethylene (12.2 %) most abundant. There was little change in the composition of polymers in the sludge over time. Overall, we found that Fenton's reagent coupled with μ-FTIR is an effective approach to characterize MPs in WWTP sludge, and that sludge could serve as a source of MPs to the environment depending on its disposal.

1. Introduction

Cumulative generation of plastic waste was estimated to be 6300 million tons between 1950 and 2015 with only 9 % recycled and 12 % incinerated, leaving nearly 80 % to accumulate in landfills or in the natural environment [1]. In recent years, microplastics (MPs), either from manufacturing or fragmentation of mismanaged plastic waste, have attracted increasing scrutiny due to concerns about their widespread occurrence in the environment and their potential threat to organisms and human health. Wastewater treatment plants (WWTPs) receive wastewater, including sewage from domestic sources, discharge from industrial operations, stormwater runoff, or some combination thereof, which characteristically contains MPs [2]. In the WWTP, the majority of these MPs are transferred to sludge through surface skimming and sedimentation [2]. Several studies have found high concentrations of MPs in waste sludge from municipal WWTPs, with one measuring MPs as high as 10,380 particles/g [3]. Although the biosolids may be further treated (e.g., anaerobic digestion, aerobic digestion, stabilization, and composting) before use as a fertilizer, the treatments have minimal effect on MPs therein [4–6]. Thus, WWTP-derived biosolids used as fertilizer are an important source of MPs to the natural environment [7,8].

Quantification of MPs in sludge is challenging because the matrix is complex, consisting of a mixture of organic matter from human waste, inorganic solids, food waste, trace chemicals, heavy metals, microorganisms, medicines, and other micropollutants. Currently, several extraction methods have been proposed to maximally remove organic matter and minimally compromise MPs, including acid-based digestion [9], alkaline treatment [4,10], and oxidative digestion [11–13]. Strong acids and bases are rarely used to extract MPs from WWTP-derived samples because of their capability to damage certain plastics such as PLA [14–16]. Hydrogen peroxide (H_2O_2) has also been employed to

* Corresponding author.
E-mail address: cizdziel@olemiss.edu (J.V. Cizdziel).

https://doi.org/10.1016/j.jece.2023.109671
Received 8 December 2022; Received in revised form 11 February 2023; Accepted 10 March 2023
Available online 11 March 2023

remove natural organic matter in samples freeing MPs for subsequent analyses, with Fenton's reagent shortening the treatment time and improving the effectiveness of the digestion protocol [16–18]. As the types of MPs in the environment is so varied, it is of importance to systematically assess the effects of different digestion schemes on a wide range of polymers.

Once extracted from the matrix, MPs can be detected and characterized by a number of analytical methods, including microscopy [19], spectroscopy [10], and thermal-based techniques [20], with vibrational spectroscopy (IR and Raman), most commonly used to identify the type of polymer. Reviews on MPs in WWTP have detailed such analytical approaches [21]. A low-cost method for detection of MPs involves fluorescence measurements after staining with dyes, such as Nile red [22]. The staining increases the degree of automation and quantification efficiency, but can lead to over estimation if non-plastic particles also bind the dye. Thus, matrix digestion and density separation, along careful inspection of fluorescing objects to not count items that are clearly not plastic or that have biological features such as spines or striations, is required [23].

Regardless of the technique employed it is critical to recover and isolate the MPs from complex environmental and biological matrices. MP extraction efficiency has been assessed through determining recovery rates of homemade or commercially available polymers spiked into samples [5,19,24,25]. However, spiked MPs are typically larger than the majority of those found in the environmental samples. Fluorescent MPs are also employed in recovery experiments because they are relatively easy to detect, but only certain morphologies (e.g., beads) and types of polymers (e.g., polyethylene) are commercially available. To increase the availability of different types and morphologies of fluorescent polymers, we previously optimized labelling a diverse group of homemade MPs with fluorescent dyes for detection, recovery, and degradation experiments [26]. However, the durability of Nile red-stained MPs in digestions to remove natural organic matter is unknown, and if the digestion process diminishes the intensity of the Nile red fluorescence it would limit its application.

In this study, we employed Nile red to stain polymers of different types and shapes, and investigated the influence of different digestion schemes, including one acid digestion protocol [(1:1 (v:v) H_2O_2 (30 wt %) + H_2SO_4 (96 wt%)), two alkaline digestion protocols (1 M NaOH and 10 % KOH), and two H_2O_2 based digestion protocols (30 % H_2O_2 and Fenton's reagent), on the fluorescence intensities of the stained MPs. The purpose was to assess whether such Nile red stained MPs can be widely used as labeled standards in experiments involving digestion of samples rich in organic matter. We also examined the alterations of physical and chemical characteristics of the stained MPs after the digestions to further assess their applicability. We then applied Fenton's reagent, which had the least impact on the MPs and effectively removed the matrix, to extract and assess the MP profiles in sludge from a modern (closed loop reactor) WWTP at University of Mississippi. Thus, this report also includes information on the sizes, shapes, abundances, and types of MPs in the sludge which was obtained between November 2019 and September 2021 under different flow regimes.

2. Materials and methods

2.1. Method validation

2.1.1. Polymer samples and characterization

Eighteen polymers were selected for analysis based on their global production, frequency of occurrence in the environment, and their use in previous studies (Table S1), including acrylonitrile-butadiene-styrene (ABS), cellulose acetate (CA), crumb rubber (CR), ethylene-vinyl acetate (EVA), expanded polystyrene foam (EPS), high-density polyethylene (HDPE), medium-density polyethylene (MDPE), low-density polyethylene (LDPE), linear low-density polyethylene (LLDPE), nylon 6,6 (PA66), polycarbonate (PC), polyester (PEST), polyethylene terephthalate (weathered PETE and PET), polylactic acid (PLA), polypropylene (PP), polystyrene (PS), and polyvinyl chloride (PVC). PC particles were cryogenically ground from large plastic debris. PLA particles and PETE films were cut with a scissor from a 3D printer PLA filament and a water bottle, respectively. The remaining plastics were obtained from Hawaii Pacific University's Polymer Kit 1.0 marketed to "harmonize plastic pollution research". These standardized MPs tend to be larger MPs (>500 μm) which improves size and mass measurements and affords great visibility of surface changes.

We characterized the polymers before and after administering the digestion protocols using microscopy, fluorescence, spectroscopy, mass measurements, and thermal methods. For fluorescence, we observed that staining the polymers by 2 μg/mL Nile red dye (prepared with DI water) at 70 °C for 3 h yielded strong fluorescent signals. These stained MPs were weighed and imaged before and after digestions using an analytical balance and a stereomicroscope (SteREO Discovery V12; Carl Zeiss Jena GmbH, Germany) equipped with a channel fluorescence (Cy3/Rhod/RFP) and an X-Cite 120Q fluorescence lamp illuminators. The fluorescence range was chosen: red (excitation at 545/25 nm, emission at 605/70 nm) with exposure time of 490.2 ms. The fluorescence intensities and fluorescing areas of the stained MPs were obtained through ImageJ software. We assessed changes in surface characteristics using attenuated total Reflection-Fourier transform infrared spectroscopy (ATR-FTIR) with an Agilent Cary 600 (Agilent Technologies, CA, USA). Spectra were collected from 600 to 4000 cm^{-1} with 32 scans at a resolution of 4 cm^{-1}. Thermal stability was measured by thermal gravimetric analysis using a TGA 550 (TA Instruments, DE, USA). Thermograms were collected between 30 and 900 °C at 20 °C/min under nitrogen.

2.1.2. Digestion tests

Nile red (Technical grade, Sigma-Aldrich) stained MPs were exposed to five different digestion schemes (Table 1). The mixture of 1:1 (v:v) H_2O_2 (30 wt%, 97 % purity, Fisher Scientific, Hampton, NH, USA): H_2SO_4 (93–98 wt%, trace metal grade, Fisher Scientific) was used after it cooled down to room temperature (22 °C). 1 M NaOH (Pellets pure, MilliporeSigma), 10 % KOH (pellets/certified ACS, Fisher Scientific), 30 % H_2O_2 and Fenton's reagent were directly mixed with sludge samples.

Samples were subjected to 10 mL 30 % H_2O_2 and 5 mL of Fenton's reagent consisting of 0.05 M Fe(II) solution (ACS reagent, Sigma-Aldrich) containing 0.6 % of concentrated sulfuric acid. After digestion, MPs were removed from 15 mL centrifuge tubes, thoroughly rinsed with DI water, and dried in Petrislide dish at laminar hood for analysis. Three replicates consisting of three particles for each polymer were subjected to each digestion protocol, except for CA and PEST that were weighed (~10 mg and ~1 mg, respectively) due to their small sizes.

2.2. Sludge sampling and analysis

2.2.1. Sludge sampling

Primary sludge, dewatered sludge, and surface scums were sampled

Table 1
Reagents and conditions for the selected five digestion protocols.

Digestion Scheme	Reagents	Conditions	References
I	30 %H_2O_2:96 %H_2SO_4 at 1:1 (v:v)	22 °C for 24 h	[9]
II	1 M NaOH	60 °C for 24 h	[4,10,16]
III	10 % KOH	60 °C for 24 h	[4,16]
IV	30 % H_2O_2	60 °C for 24 h	[6,11,13]
V	Fenton's reagent (H_2O_2:Fe(II) = 2:1(v:v))	22 °C for 24 h	[11,46]

from a WWTP that serves the University of Mississippi, home to ~23,000 students. The WWTP, as well as the abundance and characteristics of MPs in the wastewater as it flows through the different treatment compartments during different flow regimes were previously described [27]. Briefly, the wastewater from the university community is processed by a grit chamber, closed loop reactors, secondary clarifiers, and UV light before discharge. Primary sludge from the grit chamber is collected and disposed separately. The scums floating in secondary clarifiers are removed using skimmers and are discharged to scum troughs. Waste activated sludge are aerobically digested before being dewatered by a filter press. Daily flow rate to this WWTP depends highly on the on-campus population, and ranged from 679 m^3/d during a semester break to 2500 m^3/d during major sporting event (Table S2). Sludge was collected with 1 L glass jars and stored at 4 °C until analysis. All glass jars were rinsed with deionized water and heated at 450 °C for 3 h before being used.

The moisture and organic matter content were measured at 105 °C for 24 h and 550 °C for 4 h, respectively, in a muffle furnace.

2.2.2. Organic matter removal efficiency

The five selected MP extraction protocols were examined for the removal efficiency of organic matter. 5 g (wet weight) of dewatered sludge collected on 7 September 2021 was weighed into 1 L glass jars and 45 mL solution (digestion scheme I-V, Table 1) was added. Following digestion for 24 h, the mixtures were filtered through 45 μm mesh sieve and the retentate was transferred to pre-weighed 50 mL centrifuge tubes and dried at 40 °C until weight did not change. The mass loss of samples before and after treatments were calculated gravimetrically and were wholly attributed to the reduction of organic matter. Wet sludge was used for digestion because dried sludge typically contains hardened and clumped clay-like material that are not readily digested [18].

2.2.3. Microplastic extraction

Fenton's reagent was determined to be applied to extract MPs from ~5 g (wet weight) of sludge or surface scums. Weighed samples were digested with Fenton's reagent. After digestion for 3 h, samples were filtered through 45 μm mesh sieve and retentates were transferred to 250 mL glass jars with 1.6 g/cm^3 $ZnCl_2$ solution (>99 % purity, Fisher Scientific, Hampton, NH, USA) for density separation. 80 mL of $ZnCl_2$ solution was added. The mixture was stirred with a glass rod for 2 min and 20 mL was further used to rinse the MPs on the wall of glass jars down to the solution following by settling for 3 h. The top (floating) layer of debris was transferred into a glass vial using a 5 mL glass pipette. The procedure of density separation was repeated twice more. Collected floating debris were re-sieved through a 45 μm mesh screen and successively rinsed with 1 % of HCl solution and DI water. The particles on the screen were filtered through polycarbonate filters (47 mm diameter). The addition of several drops of HCl was to dissolve $ZnCl_2$ floc which formed in the dilution process of $ZnCl_2$ solution.

Five positive and six negative controls were performed along with sludge samples. 100 mL DI water was used for procedural blanks. MPs used for positive control were chosen according to the occurrence of polymers in the analyzed sludge samples. Ten particles each of commercially available fluorescent PE microbeads (150–180 μm), Nile red stained polymers (PA fibers (250–500 μm), PC fragments (250–500 μm), PETE films (500–1000 μm), PEST fibers (1–2 mm in length), green PS fragments (250–500 μm), and white PVC fragments (250–500 μm)), and non-fluorescent polymers (orange PLA fragments (250–500 μm), blue PP fragments (250–500 μm)) were spiked into 5 g of dewatered sludge collected on 7 September 2021 (Table S5). PA fibers, PC, PLA, PP, PS, and PVC fragments were cryogenically ground. PETE films and PEST fibers were cut with a scissor. Both positive and negative controls underwent identical digestion (Fenton's reagent) and density separation processes. The recovery efficiency of each polymer (Eq. 1) was used to evaluate the selected method.

$$Recovery\ efficiency = \frac{Number\ of\ each\ polymer\ \ recovered}{Number\ of\ each\ polymer\ spiked} \times 100\% \quad (1)$$

2.2.4. Microplastic observation and identification

Each extract was visually inspected at 40 × magnification using the stereomicroscope described earlier. The MP profile was documented, including morphology and major dimension. Putative MP particles were categorized as either fibers, fragments, microbeads, films or glitter. Fluorescent particles in negative controls were observed under the red fluorescence range as discussed.

To identify polymer compositions, MPs on the polycarbonate filters were transferred to 5 mL 50 % ethanol via sonication. 1 mL aliquot was filtered through 25 mm gold-coated polycarbonate track-etched filters (25 mm diameter, 0.4 μm pore size; Sterlitech Corp., Kent, WA, USA). Eight 1 mm × 1 mm sections were randomly selected on each filter and analyzed by μ-FTIR using a Perkin Elmer Spotlight 200i (Perkin Elmer, Waltham, MA, USA). Measurements were conducted in the reflectance mode using a mercury cadmium telluride (MCT) detector. Spectra were taken at 24 scans with wavelengths between 600 and 4000 cm^{-1} and a spectral resolution of 4 cm^{-1}. Sample spectra were compared to the spectra library supplied by Perkin Elmer; matches were deemed positive with > 70 % similarity between samples and library spectra [6]. Large plastic debris extracted from secondary clarifier scums were identified with μ-ATR-FTIR using a Bruker LUMOS II microscope with a liquid nitrogen cooled MCT detector (Bruker Corporation, Billerica, MA, USA). ATR spectra were obtained at the scan number of 12 scans and the spectral resolution was 4 cm^{-1}. Sample spectra were compared to the spectra library supplied by Bruker.

To minimize MP contamination, we wore bright orange-dyed cotton laboratory coats and covered samples and associated assemblies with aluminum foil when not being actively processed. The entire MP extraction process was conducted in a clean laminar flow hood.

2.3. Data analysis

All the data were the mean values (± standard deviation, SD) of replicas. Significant differences of physical and chemical changes of stained MPs were analyzed through independent-samples T test. One-way analysis of variance (ANOVA) followed by Fisher's last significant different test (LSD) was used to evaluate the difference of MP abundances in the sludge samples collected from different compartments. All statistics were calculated using SPSS version 27.0 software.

3. Results and discussion

3.1. Method optimization

3.1.1. Influence of digestion protocols on Nile red stained polymers

The red fluorescence intensities of LDPE, LLDPE, MDPE, HDPE, PP and PLA were slightly affected by acid digestion. However, PEST that was typically found in the environment showed much weaker fluorescence after acid digestion (Fig. S1). For the alkaline digestions (1 M NaOH and 10 % KOH), red fluorescence intensities of CA, PC, PETE, PEST, and PET decreased sharply, appearing dim after treatment; PE, PS, PP and PA66 were only slightly affected; and there was no effect on EVA, ABS, EPS and PVC (Fig. S1). Karakolis et al. [28] (2019) also found the decrease of red fluorescence intensity when MPs exposed to 4 M KOH solution. Polymers show variable fluorescence intensities at different pH values, which can be associated with changing charge density on the polymer surface since Nile red is protonated only in very acidic environments (pH <4.0) [29–31].

Apart from fluorescent signals, digestion protocols had other effects on certain polymers, although most of them were not substantially affected. PA66, CA and CR were seriously to completely degraded in the mixture of 1:1 (v:v) H_2O_2 (30 wt%) + H_2SO_4 (96 wt%) solution,

impacted primarily by the H_2SO_4. Apparently changes in mass and surface area for other polymers subjected to acid digestion were not observed (Table S3, S4). After treatments with 1 M NaOH and 10 % KOH, the surfaces of PET pellets were flatter and smoother, and their mass decreased by 5.1 % and 6.4 %, respectively (Table S3). This degradation may be attributed to the saponification of ester bonds. A decrease in surface area of 5.6 % was found on PET pellets after 10 % KOH treatment (Table S4). Smaller PET particles (~130 μm) were more sensitive to alkaline digestions [18]. For PC MPs, we observed little to no changes in mass or surface area with alkaline digestion. However, the development of a matte texture and weight loss was observed for PC due to hydrolytic degradation by Hurley et al. [16], and a more pronounced degradation of PC was found while using higher concentrations of NaOH solutions [14,16,32].

Biodegradable PLA pellets subjected to alkaline digestion were severely depolymerized (Fig. S2; Table S3, S4). Due to the small size of CA used in this study, the influence of five digestion protocols was assessed through the changes of size distribution. Before digestion, the size of CA was 399.02 ± 122.44 μm and significantly decreased to 239.60 ± 76.32 μm and 281.622 ± 99.41 μm following 1 M NaOH and 10 % KOH digestion, respectively ($p = 0.002$, $p = 0.005$, Table S4). The reason was that alkaline solutions caused hydrolysis of the acetate ester to hydroxyl groups, especially at high temperatures.

For 30 % H_2O_2 digestion, we did not observe significant changes in the intensity of fluorescence of the polymers, except for MDPE, HDPE, CA and PLA. The quantum yield for Nile red in 30 % H_2O_2 (pH= 4.7) is expected to be relatively constant between pH 4 and 9 [29]. However, the oxidation of both Nile red and the polymers themselves by 30 % H_2O_2 as well as the modification of surface charges of the polymers, primarily caused the changed adsorption kinetics of Nile red, can result in the decrease of fluorescence intensities. For example, the carbonyl index of stained HDPE was 0.0224, but changed to 0.0308, 0.0282, 0.0637 and 0.0451 following 1 M NaOH, 10 % KOH, 30 % H_2O_2, and Fenton's reagent treatments. Only CA was observed to undergo a decrease of fluorescent signal after being treated by Fenton's reagent, but the decrease was modest and the particles were still visible.

In the 30 % H_2O_2 digestion treatment, all PA66 particles showed cracks but otherwise no mass related changes (Fig. S3; Table S3, S4). The diffusion of oxygen radicals may facilitate the thermo-oxidative degradation of PA66 [33,34]. CR particles were severely degraded by 30 % H_2O_2, with around 25 % of mass loss (Fig. S3; Table S3, S4). Belone et al. [35] observed surface changes and modifications of physical characteristics (e.g., tensile and thermal properties) of styrene butadiene rubber after 30 % H_2O_2 digestion at 30–40 °C for a couple of days. CR is susceptible to attack by oxidants due to the double bonds in the structure. Therefore, thermo-oxidation is the likely degradation mechanism for CR. We did not find any noticeable morphological and mass changes on other tested polymers. Fenton's reagent consisted of 30 % H_2O_2 and Fe(II) but no degradation was observed (Table S3, S4). However, this exothermic reaction may cause aggregation of polymers with low glass transition temperatures.

FTIR spectra of few treated polymers were altered compared to reference spectra (Fig. S4). The 1750 cm^{-1} band of virgin CA spectrum, assigned to C═O groups, has the highest intensity, which is highly diminished after treatments, especially for 1 M NaOH digestion. In addition, substantial decreases of band intensity at 1250 cm^{-1} and 1040 cm^{-1} assigned to C-O stretching were observed [36]. This is explained by the partial hydrolysis of acetyl groups, but it can be also due to the hydrolysis of the polymer chains [37]. Consistent with FTIR results, TGA curves of treated CA particles deviated from reference material and the initial degradations of treated CA particles started at lower temperatures (263–323 °C) compared to untreated particles (336 °C) (Fig. S5).

Modifications of CR spectrum intensities at 2850–2950 cm^{-1} (-CH_2 stretching) and 1560 cm^{-1} for acid digestion and 30 % H_2O_2 treatment were observed (Fig. S4). Relative weak intensities of –CH bending at 1426 and 1370 may suggest the breakage of polymer chains. Generally, it is challenging to identify CR undergone acid and 30 % H_2O_2 treatments as characteristic peaks were almost disappeared. Besides, distinct TGA curve was observed on CR subjected to these two treatments. Although surface morphological modification was observed on PA66 particles that were subjected to 30 % H_2O_2, we did not find significant IR spectrum deviation (Fig. S4). The intensity of C═O stretching of PC particles at 1766 cm^{-1} increased following acid and 30 % H_2O_2 treatments, but this minor change would not affect the identification of PC.

PET subjected to acid digestion showed weak stretching of -CH_2 at 2960 cm^{-1} and 2910 cm^{-1} (Fig. S4). Part of C═O bond at 1720 cm^{-1} and C═C bond at 1560 cm^{-1} were broken by the oxidation of H_2SO_4. These modifications on PET could affect its identification. Due to the presence of ester bonds leading to chain scission, hydrolysis degradation slightly occurred after alkaline digestion as the peak in the region of 3430 cm^{-1} related to OH end groups slightly increased compared to untreated PET pellets. Additionally, the band at 1716 cm^{-1}, a C═O bending, was much broader in PET pellets. Nevertheless, those spectral changes were not suspected to hamper polymer identification. TGA curves did not show remarkable differences between the reference and treated PET pellets, except for acid digestion. The oxidations of PLA subjected to acid and 30 % H_2O_2 digestions were evident from the increased intensity of the band for the stretching of C═O at 1741 cm^{-1}. More obvious difference was found on TGA curves for PLA pellets. The onset temperatures for treated PLA pellets were lower than 350 °C, but it was approximately 370 °C for the reference.

3.1.2. Organic matter removal efficiency

As discussed in the methods section, we applied a filtration step using a 45 μm sieve after each digestion protocol which allowed some small undigested particles to be removed, but retain our targeted MPs (>45 μm). Thus, the total mass loss of sludge is somewhat higher than reported in previous studies [16,18]. The highest weight loss was observed by applying 30 % H_2O_2 at 60 °C for 24 h, followed by Fenton's reagent, 1:1 (v:v) H_2O_2 (30 wt%) + H_2SO_4 (96 wt%), 10 % KOH, and 1 M NaOH (Table 2). Alkaline digestions yielded some residual agglomerated sludge that although softened did not separate into particles < 45 μm, which could be a reason for their slightly lower removal efficiencies. While alkaline conditions can be effective at destroying proteins in the sludge, cellulose, chitinous materials, and humins are resistant to alkaline digestion [38,39]. Regarding that the weight loss was attributed to the removal of organic matter, we obtained > 90 % of organic matter reduction after acid, 30 % H_2O_2 and Fenton's reagent treatments.

In combination with the observed damages of the tested polymers subjected to five treatments, Fenton's reagent was the best overall protocol effectively removing organic matter, freeing the MPs without damaging them. Thus, we chose Fenton's reagent for our study of MPs in sludge from the University of Mississippi WWTP.

3.1.3. Method validation

We spiked Nile red stained plastic particles, commercially available microbeads and colored MPs to sludge collected from the University of Mississippi WWTP. Samples were processed with Fenton's reagent for removal organic matter and 1.6 g/cm^3 $ZnCl_2$ solution for density

Table 2
Total weight loss and corresponding organic matter removal efficiency for each digestion protocol.

Protocols	Total weight removal (%)	Organic matter removal (%)
1 M NaOH	84.4 ± 1.6	78.2 ± 2.2
10 % KOH	85.0 ± 2.2	79.1 ± 3.1
30 % H_2O_2	99.1 ± 0.4	98.8 ± 0.5
Fenton's reagent	95.1 ± 0.6	93.1 ± 0.8
H_2O_2:H_2SO_4 (v/v = 1:1)	93.0 ± 3.4	90.2 ± 4.7

separation. Colored fragments (PLA and PP) of 250–500 μm were accurately counted under stereomicroscope, giving recoveries of 100 % and 96 %, respectively. If smaller sizes were selected for spiking, it would be challenging to distinguish the spiked ones from MPs in sludge. The recovered MPs showed strong red fluorescence intensities, facilitating their enumeration (Fig. S6). PE microbeads and PETE films exhibited 100 % of recovery rates, followed by PC (98 %), PS (92 %) and PVC fragments (94 %). PA and PEST fibers showed slight lower recovery (90 % and 87 %). Unlike other morphologies, fibers were able to longitudinally pass through 45 μm sieve due to their fine width and good flexibility [40,41]. Additionally, their relatively large surface area allowed them to easily attach to the glass wall or sludge floc [42]. Overall, we obtained satisfied recoveries for all spiked MPs.

Negative blanks were universally contaminated with particles ranging from 12 to 26 particles/blank sample. Fibers accounted for the majority and may be associated with the atmospheric fallout and face masks as the most of commercially available face masks are made of synthetic polymers (e.g., PS, PAN, PE, PU and PEST). The reported MP abundances in the sludge samples were blank subtracted.

3.2. Occurrence and characteristics of microplastics in the sludge

3.2.1. Microplastic abundances

MPs extracted from sludge samples ranged from 13.2 ± 3.8 particles/g to 380.0 ± 46.4 particles/g (dry weight), with an average of 159.4 ± 118.8 particles/g (Fig. 1). However, a great number of studies found significantly lower MP abundances in the sludge collected from municipal WWTPs. An average of 4.2–15.4 particles/g of MPs were extracted from sewage sludge undergone treatment including thermal drying, anaerobic digestion and lime stabilization [5]. Pittura et al. [43] found 1.0–5.3 particles/g of MPs in sludge collected from different stages. The combination of wastewater sources, WWTP operations, and detection methods affects the detected MP abundances. MPs in the primary sludge and dewatered sludge collected during holidays and off-campus periods were significantly lower than those during on-campus study periods and sport events ($p = 0.001$, $p = 0.029$), which suggested that the on-campus population substantially influenced the MP abundance in the sludge.

At the University of Mississippi WWTP, surface scums and sludge in the primary settling chamber are collected separately. We observed the lowest concentration of MPs in the primary sludge in comparison to surface scums from secondary clarifiers and dewatered sludge ($p = 0.001$ and $p < 0.001$), which mainly consisted of sand and other inorganic materials (Table S2). Although we did not measure the oil/grease/surface scums of this chamber, others have found abundant MPs at the skimming troughs of primary tank [2,44]. High abundances of MPs were found in the scums of secondary clarifiers, ranging from 61.2 to 511.6 particles/g. This also corroborated that the majority of MPs were trapped by surface scums.

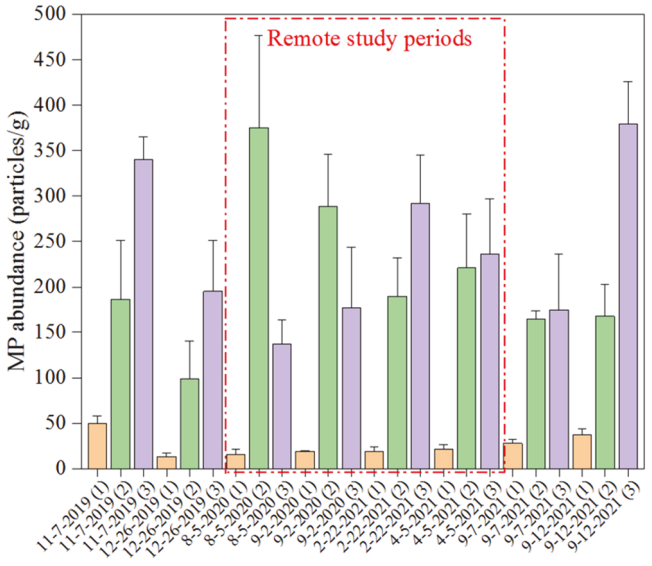

Fig. 1. MP abundance in the sludge collected at different periods. (1), (2), and (3) denote primary sludge, secondary clarifier scums, and dewatered sludge, respectively.

MP abundance in the dewatered sludge was positively correlated with the influent flow ($r = 0.789$, $p = 0.02$). In addition, dewatered sludge contained high abundances of MPs even during low flow periods when students were off-campus on remote study due to the pandemic. Whereas the overall amount of sludge generated decreased, the age of the sludge in the system increased allowing capture and buildup of MPs during the longer process times. Due to the relative lack of incoming raw sewage to fully support the microorganisms, the plant increased the return ratio of activated sludge to maintain healthy reproduction of microorganisms. Upon return to campus, MP concentrations in the sewage water and in the water of the different WWTP compartments varied. For example, just after football games when the campus population may be several times higher than normal, higher MP concentrations are observed.

We estimate that 7.76×10^{10} particles are discharged annually in dewatered sludge sent to a landfill by the University of Mississippi WWTP based on the average concentration of 141 particles/g and the annual sludge amount of 550.5 t. Dewatered sludge or biosolids containing MPs are also routinely used as fertilizer for agriculture, but that can result in MP pollution in runoff from the agricultural field [8]. Application of sludge to land contributes ~7.40×10^{12} particles/day to the terrestrial environment in the UK [46]. Corradini et al. [7] found that MP abundance was significantly higher in the fields that underwent sludge applications.

3.2.2. Morphological characteristics and size distribution

Fibers were predominant in all sludge samples (37–65 %), followed by fragments (13–32 %) and films (11–24 %) (Fig. 2). As fibers are light and tend to have relatively large surface areas, activated sludge is even more prone to capture them compared to other shapes. Potential sources for synthetic fibers include the laundering of fabrics and shedding of textiles. Together with synthetic fibers, a large variety of fibers made of natural polymers (e.g., wool, linen, and cotton) deposit to sludge. Natural polymers are not included in MP studies, but their anthropogenic character and presence additives could be a hazard to the natural environment [6]. It's challenging to track the sources of MP fragments and films since they could be formed before entering the WWTP and by wastewater treatment processes. Foams, microbeads and glitter were sporadically observed in the sludge. Cosmetics and personal care products contain microbeads or fragments as exfoliating agent or specific medical application [2,47]. Glitter, rarely reported in the aquatic environment, is currently being considered in the ban on MPs in personal care and cosmetic products in some countries; it is primarily made of PET (1.30–1.40 g/cm^3) and therefore is typically found in the sludge [4,

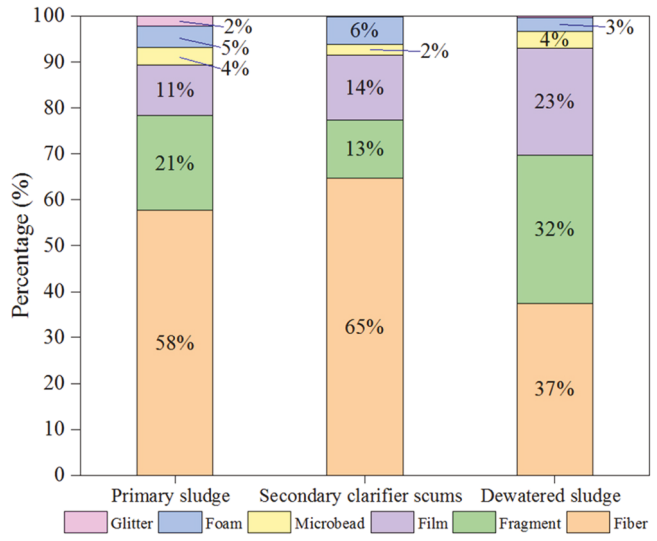

Fig. 2. MP morphological distribution in the sludge collected from different stages.

25,43,44]. Only 0.08–2.1 % of MPs were classified as glitter in this study with the average size of 328.0 ± 292.0 μm, which was similar to WWTPs in Norway [4] and Italy [43]. Glitter discovered in WWTPs can be attributed to cosmetics, nail polishes, fabrics and decorations for celebrations. The fine surface metal coating of glitter could be preferentially released to ambient environment during the weathering process.

Primary sludge had a relatively higher proportion (~20 %) of large MPs (1–5 mm) compared to other types of sludge samples (Fig. 3). This is likely because these larger and heavier MPs tend to be less influenced by the turbulent flow and can settle in the grit chamber. Nevertheless, the highest concentration of MPs in the primary sludge was in the 250–500 μm size range, with most being fragments, films, foams and glitters (Fig. 3).

Surface scums in the secondary clarifiers also contained a fair number of plastic debris, some of which were mesoplastics (5–10 mm) and macroplastics (>10 mm). On average, 9.9 ± 5.1 particles/g of plastic debris were found, with 55.8 % being fragments (Fig. S7). A relatively high proportion of microbeads were also observed (21.5 %). It was noticed that PE microbeads were efficiently removed together with grease from the surface of wastewater [44,48]. Films seemed to stem primarily from the breakdown of package bags (Fig. S8), which could

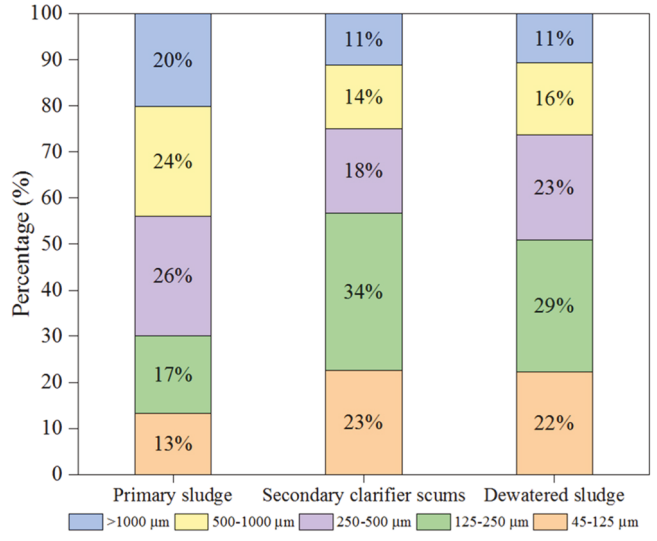

Fig. 3. MP size distribution in the sludge collected from different stages.

happen during the wastewater treatment process. The relatively high proportion of meso- and macro-plastics in the secondary clarifier surface scums is likely because small MPs are more prone to be entangled by activated sludge. The average size of microbeads was 732.8 ± 194 μm, which was significantly larger than the microbeads found in the sludge (75.1 ± 31.2 μm). Based on Euromonitor data, it has been estimated that ~6 % of all liquid soaps still contain microbeads and ~70 % of those microbeads are > 450 μm [49].

3.2.3. Polymer composition of microplastics in the sludge

MPs extracted from sludge collected from different compartments were identified with μ-FTIR. PEST, PA and PE were the most abundant polymers in the sludge from the different stages with the occurrence of other polymers at lower and more variable levels (Fig. S9). As PEST and PA are ubiquitous in textiles, clothing, carpets and toothbrushes, and denser than wastewater, it is common to observe these polymers in the sludge [13,25,48,50,51]. Studies reported over 1900 [52] and 110,000 [53] fibers released by a single garment. The removal of MPs from wastewater to sludge mainly depends on their densities and as a result, denser polymers are frequently found in sludge, such as PET (6.4 %), PVC (5.5 %), PMMA (4.6 %), and PC (3.6 %) (Fig. 4). Higher abundances of PET in dewatered sludge than in the effluent has been previously reported [25]. Low-density polymers (e.g., PE, PS and PP) were also found in the sludge and surface scums (Fig. 4, Fig. S9). The extracellular polymeric substances excreted by microorganisms, added flocculants, and adhesion to denser particles facilitate precipitation of these low-density polymers [2]. Irregular shaped blue PE fragments (~140 μm) was commonly found in the sludge (Fig. S8B), which may originate from toothpaste or cleanser scrubs [2,48]. Carr et al. [2] also observed randomly shaped PE fragments that tended to settle or associated with biofilms.

As it is challenging to reliably identify fibers with ATR-FTIR [10,54], we only used the technique to identify other shapes (fragments, beads, foams, and films) of the larger plastic debris. The majority of debris were fragments (55.8 %), followed by microbeads (21.5 %), films (16.6 %) and foams (6.1 %). Large debris extracted from secondary clarifier scums are expected to have lower densities than wastewater, since they are less affected by biofouling or ambient conditions and buoyant on the wastewater. Using ATR-FTIR the most abundant polymer was PE, which is consistent with its high use in consumer products and its high global production and consumption. Microbeads in personal care products can still be found on store shelves despite their being banned in many countries. The beads are primarily made of PE and PP, which are positively buoyant in the wastewater and thus are likely to float on the surface of wastewater where they can be skimmed off with surface scums. We found all microbeads among the secondary clarifier scums were PE. We also found blue fragments among the large debris that were probably from face masks after comparing to the electron microscopy image of outer layer of medical face mask [55,56] and were identified as composed of PP (Fig. S8H). EPS foams accounted for 5.3 %, which may be associated with the extremely low density (0.015–0.03 g/cm^3).

4. Conclusions

Compared to H_2O_2 based protocols, alkaline digestions were less effective at removing organic matter in the sludge and altered some plastics (e.g., CA, PET, and PLA). Acid digestion was aggressive to CA, CR, and PA damaging the MPs. 30 % H_2O_2 treatment was most effective at removing organic matter, but resulted in serious degradation of CR particles. Fenton's reagent was relatively friendly to all tested polymers and had little impact on the fluorescent intensities of Nile red stained polymers. Therefore, Fenton's reagent is suitable to extract MPs from samples abundant in organic matter, such as WWTP sludge, and Nile red stained MPs can be used to assess sample pretreatment (spike recovery experiments) when using Fenton's reagent.

Using Fenton's reagent to extract MPs and a combination of

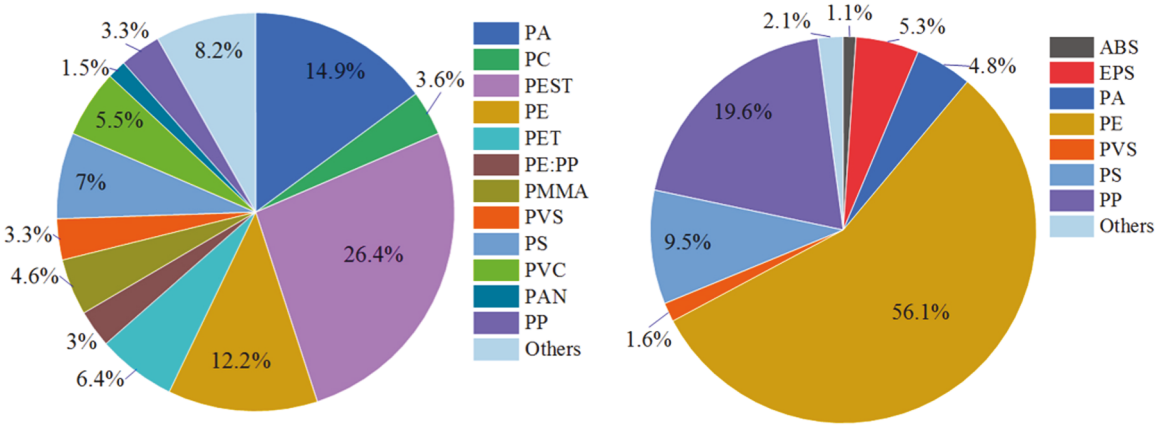

Fig. 4. Polymer compositions of microplastics in the sludge (primary and dewatered sludge combined) (A) and in the secondary clarifier scums (B). PAN: Polyacrylonitrile; PVS: Polyvinyl stearate; PMMA: Poly (methyl methacrylate). Other abbreviations were described in Section 2.1.1. A comparison between the MP profiles of the primary and dewatered sludge is given in Fig. S9.

stereomicroscopy and μ-FTIR to quantify and identify the MPs, we observed that MP concentrations in primary sludge and dewatered sludge from the University of Mississippi WWTP were significantly lower during periods with low populations on-campus (between semesters) compared to when populations on campus were higher (during the semester and sporting events). However, there were higher MP abundances in surface scums of secondary clarifiers during periods with low on-campus student populations, likely due to the longer wastewater process time established during the low-flow period. Therefore, researchers should not neglect the contribution of surface scums when determining the fate of MPs in WWTPs. Across sample types, the extracted MPs were mainly fibers, followed by fragments and films. Microbeads and glitter were sporadically observed. Consistent with other studies, the most abundant polymers were PEST, PE and PA (nylon). Denser polymers (PET, PMMA and PVC) were also frequently observed. MP debris extracted from secondary clarifier scums were primarily composed of low-density plastics (PE, PP and PS). The abundance of MPs in the sludge suggests that sludge could serve as a source to different environmental compartments depending on its reuse or disposal. Further work should focus on strategies to enhance MP removal, especially for the most abundant polymers (e.g., PEST and PE), and on corresponding removal mechanisms.

CRediT authorship contribution statement

Zhiqiang Gao: Conceptualization, Methodology, Formal analysis, Writing – original draft. **James Cizdziel:** Conceptualization, Supervision, Writing – review & editing. **Laiguo Chen:** Writing – review & editing.

Declaration of Competing Interest

The authors declare the following financial interests/personal relationships which may be considered as potential competing interests: James Cizdziel reports financial support was provided by US Geological Survey. James Cizdziel reports equipment, drugs, or supplies was provided by National Science Foundation.

Data Availability

Data will be made available on request.

Acknowledgments

We are grateful to David Adkisson and his team at the WWTP for sampling access and information on plant operations, and Yonglin Chen for polymer identification by using μ-FTIR technique. For access to the stereomicroscope, we thank the GlyCORE Imaging Core supported by an Institutional Development Award (IDeA) from the National Institute of General Medical Sciences of the National Institutes of Health under award number P20GM103460. This project was supported by USGS 104g Grant #G16AP00065 and NSF Grant MRI-2116597. The views and conclusions contained in this document are those of the authors and should not be interpreted as representing the opinions or policies of the USGS. Mention of trade names or commercial products does not constitute their endorsement by the USGS.

Declaration of competing interests

Author James Cizdziel received funds from the USGS grant (G16AP0065) for a portion of his summer salary during the project. The funders had no role in the design of the study; in the collection, analyses, or interpretation of data; in the writing of the manuscript, or in the decision to publish the results.

Appendix A. Supporting information

Supplementary data associated with this article can be found in the online version at doi:10.1016/j.jece.2023.109671.

References

[1] R. Geyer, J.R. Jambeck, K.L. Law, Production, use, and fate of all plastics ever made, Sci. Adv. 3 (2017) 1700782.
[2] S.A. Carr, J. Liu, A.G. Tesoro, Transport and fate of microplastic particles in wastewater treatment plants, Water Res. 91 (2016) 174–182.
[3] L. Zhang, J. Liu, Y. Xie, S. Zhong, P. Gao, Occurrence and removal of microplastics from wastewater treatment plants in a typical tourist city in China, J. Clean. Prod. 291 (2021), 125968.
[4] A.L. Lusher, R. Hurley, C. Vogelsang, L. Nizzetto, M. Olsen, Mapp. Micro Sludge (2017).
[5] A.M. Mahon, B. O'Connell, M.G. Healy, I. O'Connor, R. Officer, R. Nash, L. Morrison, Microplastics in sewage sludge: effects of treatment, Environ. Sci. Technol. 51 (2017) 810–818.
[6] C. Edo, M. González-Pleiter, F. Leganés, F. Fernández-Piñas, R. Rosal, Fate of microplastics in wastewater treatment plants and their environmental dispersion with effluent and sludge, Environ. Pollut. 259 (2020), 113837.
[7] F. Corradini, P. Meza, R. Eguiluz, F. Casado, E. Huerta-Lwanga, V. Geissen, Evidence of microplastic accumulation in agricultural soils from sewage sludge disposal, Sci. Total Environ. 671 (2019) 411–420.
[8] P. van den Berg, E. Huerta-Lwanga, F. Corradini, V. Geissen, Sewage sludge application as a vehicle for microplastics in eastern Spanish agricultural soils, Environ. Pollut. 261 (2020), 114198.
[9] R. Hernández-Arenas, A. Beltrán-Sanahuja, P. Navarro-Quirant, C. Sanz-Lazaro, The effect of sewage sludge containing microplastics on growth and fruit development of tomato plants, Environ. Pollut. 268 (2021), 115779.

[10] S.M. Mintenig, I. Int-Veen, M.G. Löder, S. Primpke, G. Gerdts, Identification of microplastic in effluents of waste water treatment plants using focal plane array-based micro-Fourier-transform infrared imaging, Water Res. 108 (2017) 365–372.
[11] C.B. Alvim, M.A. Bes-Piá, J.A. Mendoza-Roca, Separation and identification of microplastics from primary and secondary effluents and activated sludge from wastewater treatment plants, Chem. Eng. J. 402 (2020), 126293.
[12] S. Cunsolo, J. Williams, M. Hale, D.S. Read, F. Couceiro, Optimising sample preparation for FTIR-based microplastic analysis in wastewater and sludge samples: multiple digestions, Anal. Bioanal. Chem. 413 (2021) 3789–3799.
[13] S.S.A. Petroody, S.H. Hashemi, C.A. van Gestel, Transport and accumulation of microplastics through wastewater treatment sludge processes, Chemosphere 278 (2021), 130471.
[14] A. Dehaut, A.L. Cassone, L. Frère, L. Hermabessiere, C. Himber, E. Rinnert, G. Rivière, C. Lambert, P. Soudant, A. Huvet, G. Duflos, Microplastics in seafood: Benchmark protocol for their extraction and characterization, Environ. Pollut. 215 (2016) 223–233.
[15] A. Karami, A. Golieskardi, C.K. Choo, N. Romano, Y.B. Ho, B. Salamatinia, A high-performance protocol for extraction of microplastics in fish, Sci. Total Environ. 578 (2017) 485–494.
[16] R.R. Hurley, A.L. Lusher, M. Olsen, L. Nizzetto, Validation of a method for extracting microplastics from complex, organic-rich, environmental matrices, Environ. Sci. Technol. 52 (2018) 7409–7417.
[17] A.S. Tagg, J.P. Harrison, Y. Ju-Nam, M. Sapp, E.L. Bradley, C.J. Sinclair, J.J. Ojeda, Fenton's reagent for the rapid and efficient isolation of microplastics from wastewater, Chem. Commun. 53 (2017) 372–375.
[18] M.S. Al-Azzawi, S. Kefer, J. Weißer, J. Reichel, C. Schwaller, K. Glas, O. Knoop, J. E. Drewes, Validation of sample preparation methods for microplastic analysis in wastewater matrices—reproducibility and standardization, Waters 12 (2020) 2445.
[19] V. Hidalgo-Ruz, L. Gutow, R.C. Thompson, M. Thiel, Microplastics in the marine environment: a review of the methods used for identification and quantification, Environ. Sci. Technol. 46 (2012) 3060–3075.
[20] E.D. Okoffo, C. Rauert, K.V. Thomas, Mass quantification of microplastic at wastewater treatment plants by pyrolysis-gas chromatography–mass spectrometry, Sci. Total Environ. 856 (2023), 159251.
[21] Z. Gao, L. Chen, J. Cizdziel, Y. Huang, Research progress on microplastics in wastewater treatment plants: a holistic review, J. Environ. Manag. 325 (2023), 116411.
[22] T. Maes, R. Jessop, N. Wellner, K. Haupt, A.G. Mayes, A rapid-screening approach to detect and quantify microplastics based on fluorescent tagging with Nile Red, Sci. Rep. 7 (2017) 1–10.
[23] A. Scircle, J.V. Cizdziel, L. Tisinger, T. Anumol, D. Robey, Occurrence of microplastic pollution at oyster reefs and other coastal sites in the Mississippi sound, USA: impacts of freshwater inflows from flooding, Toxics 8 (2020) 35.
[24] M. Simon, N. van Alst, J. Vollertsen, Quantification of microplastic mass and removal rates at wastewater treatment plants applying Focal Plane Array (FPA)-based Fourier Transform Infrared (FT-IR) imaging, Water Res. 142 (2018) 1–9.
[25] S. Raju, M. Carbery, A. Kuttykattil, K. Senthirajah, A. Lundmark, Z. Rogers, S.C. B. Suresh, G. Evans, T. Palanisami, Improved methodology to determine the fate and transport of microplastics in a secondary wastewater treatment plant, Water Res. 173 (2020), 115549.
[26] Z. Gao, K. Wontor, J.V. Cizdziel, Labeling microplastics with fluorescent dyes for detection, recovery, and degradation experiments, Molecules 27 (2022) 7415.
[27] Z. Gao, J.V. Cizdziel, K. Wontor, A. Vianello, Spatiotemporal characteristics of microplastics in a university wastewater treatment plant: Influence of sudden on-campus population swings, J. Environ. Chem. Eng. 10 (2022), 108834.
[28] E.G. Karakolis, B. Nguyen, J.B. You, C.M. Rochman, D. Sinton, Fluorescent dyes for visualizing microplastic particles and fibers in laboratory-based studies, Environ. Sci. Technol. Lett. 6 (2019) 334–340.
[29] J. Hendriks, T. Gensch, L. Hviid, M.A. van Der Horst, K.J. Hellingwerf, J.J. Van, Thor, Transient exposure of hydrophobic surface in the photoactive yellow protein monitored with Nile Red, Biophys. J. 82 (2002) 1632–1643.
[30] R. Tang, W. Ji, C. Wang, pH-responsive micelles based on amphiphilic block copolymers bearing ortho ester pendants as potential drug carriers, Macromol. Chem. Phys. 212 (2011) 1185–1192.
[31] M.T. Sturm, H. Horn, K. Schuhen, The potential of fluorescent dyes—comparative study of Nile red and three derivatives for the detection of microplastics, Anal. Bioanal. Chem. 413 (2021) 1059–1071.
[32] M.T. Nuelle, J.H. Dekiff, D. Remy, E. Fries, A new analytical approach for monitoring microplastics in marine sediments, Environ. Pollut. 184 (2014) 161–169.
[33] E.S. Gonçalves, L. Poulsen, P.R. Ogilby, Mechanism of the temperature-dependent degradation of polyamide 66 films exposed to water, Polym. Degrad. Stab. 92 (2007) 1977–1985.
[34] I. Ksouri, O. De Almeida, N. Haddar, Long term ageing of polyamide 6 and polyamide 6 reinforced with 30 % of glass fibers: physicochemical, mechanical and morphological characterization, J. Polym. Res. 24 (2017) 1–12.
[35] M.C.L. Belone, M. Kokko, E. Sarlin, Degradation of common polymers in sewage sludge purification process developed for microplastic analysis, Environ. Pollut. 269 (2021), 116235.
[36] S. Nunes, F. Ramacciotti, A. Neves, E.M. Angelin, A.M. Ramos, É. Roldão, N. Wallaszkovits, A.A. Armijo, M.J. Melo, A diagnostic tool for assessing the conservation condition of cellulose nitrate and acetate in heritage collections: quantifying the degree of substitution by infrared spectroscopy, Herit. Sci. 8 (2020) 1–14.
[37] O.S. Serbanescu, A.M. Pandele, F. Miculescu, S.I. Voicu, Synthesis and characterization of cellulose acetate membranes with self-indicating properties by changing the membrane surface color for separation of Gd (III), Coatings 10 (2020) 468.
[38] M. Bläsing, W. Amelung, Plastics in soil: analytical methods and possible sources, Sci. Total Environ. 612 (2018) 422–435.
[39] A. Herrera, P. Garrido-Amador, I. Martínez, M.D. Samper, J. López-Martínez, M. Gómez, T.T. Packard, Novel methodology to isolate microplastics from vegetal-rich samples, Mar. Pollut. Bull. 129 (2018) 61–69.
[40] S. Ziajahromi, P.A. Neale, L. Rintoul, F.D. Leusch, Wastewater treatment plants as a pathway for microplastics: development of a new approach to sample wastewater-based microplastics, Water Res. 112 (2017) 93–99.
[41] M. Lares, M.C. Ncibi, M. Sillanpää, M. Sillanpää, Intercomparison study on commonly used methods to determine microplastics in wastewater and sludge samples, Environ. Sci. Pollut. Res. 26 (2019) 12109–12122.
[42] H.J. Park, M.J. Oh, P.G. Kim, G. Kim, D.H. Jeong, B.K. Ju, W.S. Lee, H.M. Chung, H. J. Kang, J.H. Kwon, National reconnaissance survey of microplastics in municipal wastewater treatment plants in Korea, Environ. Sci. Technol. 54 (2020) 1503–1512.
[43] L. Pittura, A. Foglia, Ç. Akyol, G. Cipolletta, M. Benedetti, F. Regoli, A.L. Eusebi, S. Sabbatini, L.Y. Tseng, E. Katsou, S. Gorbi, Microplastics in real wastewater treatment schemes: Comparative assessment and relevant inhibition effects on anaerobic processes, Chemosphere 262 (2021), 128415.
[44] F. Murphy, C. Ewins, F. Carbonnier, B. Quinn, Wastewater treatment works (WwTW) as a source of microplastics in the aquatic environment, Environ. Sci. Technol. 50 (2016) 5800–5808.
[45] M. Richard, S. Brown, F. Collins, Activated sludge microbiology problems and their control. In 20th Annual USEPA National Operator Trainers Conference (Vol. 8, pp. 1–21). 2003, June.
[46] A.A. Horton, R.K. Cross, D.S. Read, M.D. Jürgens, H.L. Ball, C. Svendsen, J. Vollertsen, A.C. Johnson, Semi-automated analysis of microplastics in complex wastewater samples, Environ. Pollut. 268 (2021), 115841.
[47] K. Duis, A. Coors, Microplastics in the aquatic and terrestrial environment: sources (with a specific focus on personal care products), fate and effects, Environ. Sci. Eur. 28 (2016) 1–25.
[48] M. Lares, M.C. Ncibi, M. Sillanpää, M. Sillanpää, Occurrence, identification and removal of microplastic particles and fibers in conventional activated sludge process and advanced MBR technology, Water Res. 133 (2018) 236–246.
[49] T. Gouin, J. Avalos, I. Brunning, K. Brzuska, J. De Graaf, J. Kaumanns, T. Koning, M. Meyberg, K. Rettinger, H. Schlatter, J. Thomas, Use of micro-plastic beads in cosmetic products in Europe and their estimated emissions to the North Sea environment, SOFW J. 141 (2015) 40–46.
[50] X. Liu, W. Yuan, M. Di, Z. Li, J. Wang, Transfer and fate of microplastics during the conventional activated sludge process in one wastewater treatment plant of China, Chem. Eng. J. 362 (2019) 176–182.
[51] Q. Xu, Y. Gao, L. Xu, W. Shi, F. Wang, G.A. LeBlanc, S. Cui, L. An, K. Lei, Investigation of the microplastics profile in sludge from China's largest Water reclamation plant using a feasible isolation device, J. Hazard. Mater. 388 (2020), 122067.
[52] M.A. Browne, P. Crump, S.J. Niven, E. Teuten, A. Tonkin, T. Galloway, R. Thompson, Accumulation of microplastic on shorelines worldwide: sources and sinks, Environ. Sci. Technol. 45 (2011) 9175–9179.
[53] B.M.C. Almroth, L. Åström, S. Roslund, H. Petersson, M. Johansson, N.K. Persson, Quantifying shedding of synthetic fibers from textiles; a source of microplastics released into the environment, Environ. Sci. Pollut. Res. 25 (2018) 1191–1199.
[54] H.A. Leslie, S.H. Brandsma, M.J.M. Van Velzen, A.D. Vethaak, Microplastics en route: Field measurements in the Dutch river delta and Amsterdam canals, wastewater treatment plants, North Sea sediments and biota, Environ. Int. 101 (2017) 133–142.
[55] L.I. Xiao, H. Sakagami, N. Miwa, A new method for testing filtration efficiency of mask materials under sneeze-like pressure, In vivo 34 (2020) 1637–1644.
[56] K.G. Drouillard, A. Tomkins, S. Lackie, S. Laengert, A. Baker, C.M. Clase, C.F. De Lannoy, D. Cavallo-Medved, L.A. Porter, R.S. Rudman, Fitted filtration efficiency and breathability of 2-ply cotton masks: identification of cotton consumer categories acceptable for home-made cloth mask construction, PLoS One 17 (2022) 0264090.